測地学会誌，第52巻，第2号
(2006)，141－154頁

Journal of the Geodetic Society of Japan
Vol. 52, No. 2, (2006), pp. 141－154

Reduction of Influences of the Earth's Surface Fluid Loads on GPS Site Coordinate Time Series

Hiroshi Takiguchi[1] and Yoichi Fukuda[2]

1) Kashima Space Research Center,
National Institute of Information and Communications Technology

2) Graduate School of Science, Kyoto University

(Received January 10, 2006; Revised June 22, 2006; Accepted June 27, 2006)

GPS座標時系列におよぼす地球表層流体の荷重変動影響の補正

瀧口　博士[1]・福田　洋一[2]

1) 情報通信研究機構鹿島宇宙技術センター
2) 京都大学大学院理学研究科

(2006年1月10日受付，2006年6月22日改訂，2006年6月27日受理)

要　旨

GPS局の座標時系列には，しばしば顕著な周期変化が見られる．この原因としては，大気荷重および非潮汐海洋荷重，陸水荷重，積雪荷重など，様々な荷重の影響が考えられる．そこで，これらの荷重による局位置の変動を見積もり，GEONET（GPS Earth Observation Network）の座標時系列から荷重に伴う周期シグナルがどの程度取り除けるかを検討した．GEONETの座標時系列（F2解）は，解析ソフトウェアのバグによる誤差や，つくばのIGS点に見られるような地下水変化に伴う変動が含まれている．このため，まず，これらの影響を補正した後，いくつかの荷重の組合せでGPS局位置の補正を試みた．その結果，複数の荷重を組み合わせた場合，局位置変動の年周振幅は，水平成分，垂直成分共に2割程小さくなることが判明した．また，変動の要因としては非潮汐海洋荷重の寄与が比較的大きい事が分かった．さらに，1997年の豊後水道におけるスロースリップイベント時の時系列について荷重補正を行ったところ，スロースリップイベントの解析に荷重補正が十分有効である事が示された．

Abstract

Conspicuous periodic variations often appear in GPS site coordinate time series. These variations could be influenced by various loads, such as atmospheric, non-tidal ocean, continental water, and snow loads. To eliminate the load influences from the GPS site coordinate time series, we estimated the influences at the GEONET (GPS Earth Observation Network) sites by using meteorological and other loading data sets. Because the GEONET coordinates (F2 solution) suffer scale errors due to a software bug and groundwater variations at the International GNSS Service (IGS) station in Tsukuba, we first corrected these errors. Then, the corrections of loading influences were evaluated for several combinations of the loads. The results show that a combination of atmospheric, non-tidal ocean, continental water, and snow loads can eliminate about 20% of the annual signal in the coordinate time series for both the

horizontal and vertical components. They also show that the influence of the non-tidal ocean load is the largest of all the loads. We applied the loading correction to the data of the 1997 Bungo channel slow slip event and showed that the correction can benefit the analysis of such a non-periodic event.

1. Introduction

Temporal changes of surface loadings due to the mass redistribution of the fluid envelope of the Earth, i.e., the atmosphere, hydrosphere, and cryosphere, cause the Earth to deform and consequently change the coordinates of observation sites. The coordinate changes can be measured by space geodetic techniques such as Very Long Baseline Interferometry (VLBI) (e.g., van Dam and Herring, 1994) and the Global Positioning System (GPS) (e.g., van Dam *et al.*, 1994). For studies of crustal movements, such displacements due to the surface loadings should be eliminated. Therefore, several studies have been carried out to estimate the loading influences. van Dam *et al.* (1998, 2001) estimated crustal displacements due to the loading of the atmosphere and continental water. Mangiarotti (2001) estimated the influences of snow, non-tidal ocean, atmospheric, and soil moisture loads. He obtained the annual variation of vertical displacements and compared the estimated and observed displacements at 16 Doppler Orbitography by Radiopositioning Integrated on Satellite (DORIS) stations. Dong *et al.* (2002) extracted seasonal variations from 4.5 years of GPS coordinates and revealed that up to 40% of the annual signal of the vertical variations could be explained by combinations of the loading influences. They also evaluated the amplitudes of the annual signals and estimated that 4–10 mm is due to the atmospheric loading, 2–5 mm is due to the non-tidal ocean loading, and 3–15 mm is due to the continental water loading including snow and soil moisture.

Heki (2001, 2003 and 2004) evaluated the loading influences of various sources on the seasonal variations of GPS Earth Observation Network (GEONET) coordinates. Heki (2004) estimated the influences of snow, atmospheric, non-tidal ocean, soil moisture, and water reservoir loads in particular and concluded that the periodic variations of GPS site coordinate time series are well explained by the loading except the scale variations (systematic errors of unknown origin) suggested by Hatanaka (2003a, 2003b). Heki (2004) removed the scale variations only empirically by fitting periodic functions because the origin of the scale variation was not clear then. Later on, it was revealed that the scale variations have two origins. Munekane *et al.* (2004) found periodic variations in the time series of TSKB International GNSS Service (IGS) station at Tsukuba, installed by the Geographical Survey Institute (GSI), and the variations were found to be due to groundwater variations in the Tsukuba area. Because the GEONET coordinates use the IGS coordinates at TSKB as the reference station, their time series suffer from seasonal scale changes due to the periodic height variations of the Tsukuba region. The other reason for the scale variations is improper corrections of the solid Earth tides due to a bug in Bernese GPS software version 4.2.

Without a doubt, GPS site coordinate time series include loading influences, and they should be calculated using appropriate data sets of mass redistribution. In spite of these

efforts, the results obtained so far still do not completely explain the influence of the changing loads. Some studies (e.g., van Dam *et al.*, 1994) only estimated the amplitude of the load displacements, and others (e.g., Heki, 2004) only estimated the atmospheric loading using local meteorological data. Therefore, we tried to calculate the loading influences in a more comprehensive way and attempted to eliminate the periodic variations observed in the GEONET site coordinate time series. In this study, we first prepared the time series of displacements caused by loads using their global data sets, and in this paper, we discuss the characteristics of the load influences by comparing them with routinely provided atmospheric pressure loading data sets (Petrov and Boy, 2004; Gegout, 2004). Next, we discuss the correction of the GEONET site coordinate time series to evaluate the results. Finally, we show an example of the correction applied to time series including the slow slip event in the Bungo channel region in 1997 to see the importance of the correction in the analysis of tectonic events.

2. Calculation of the loading influences

2.1. Methodology

The deformation of the Earth's surface due to loading can be estimated by a convolution integral with Farrell's Green function (Farrell, 1972). The radial elastic deformation L is given by a global integral:

$$L(\theta',\lambda') = \rho \iint H(\theta,\lambda) G_L(\phi) T(\alpha) dS, \tag{1}$$

where ρ is the mean density of the loading material, H is the data of the mass variations, G_L is the mass-loading Green's function of displacements (Farrell, 1972), T is a combination of the trigonometric functions of the azimuth (α), and G_L is a function of the angular distance (ϕ) between the estimation point with coordinates (colatitude, longitude) = (θ',λ') and the loading point (θ,λ). For example, the Green's function for radial displacement is expressed as

$$G_L^{RD}(\phi) = \frac{R}{M_e} \sum_{n=0}^{\infty} h_n' P_n(\cos\phi), \tag{2}$$

where M_e and R are the mass and radius of the Earth, h' is the load Love number, and P_n is the Legendre function of degree n (Matsumoto *et al.*, 2001).

We used subroutine programs in Global Oceanic Tidal Correction version 2 (GOTIC2) and a high-resolution land-sea database (Matsumoto *et al.*, 2001) to calculate the displacements.

2.2. Data used for load calculation

We calculated the atmospheric loading (AL), the non-tidal ocean loading (NTOL), the continental water loading (CWL), and the snow loading (SL) influences. The details of the data sets used for the calculations are as follows.

2.2.1. Atmospheric loading influences

We used the surface pressure data of NCEP/NCAR Reanalysis 1 (Kalnay *et al.*, 1996) to estimate the AL influences. The pressure values were given in 2.5° × 2.5° grids at every 6-hour interval. We calculated the influences from January 1, 1996 to July 31, 2004.

2.2.2. Non-tidal ocean loading influences

We used Topex/Poseidon (T/P) altimetry data and ocean bottom pressure data of the Estimating the Circulation and Climate of the Ocean (ECCO) model. We use NTOL (T/P) to denote the NTOL calculated from T/P data and NTOL (ECCO) to denote the NTOL calculated from the ECCO model.

The T/P altimetry data are the sea level data from the World Ocean Circulation Experiment Satellite Data version 3.0 (1.0° × 1.0° grid with 5-day resolution from 1997–2001). The sea level data include steric height changes caused by temperature and salinity (Gill and Niiler, 1973). To remove the thermal steric influences, we used sea surface temperature (SST) data of 5-channel advanced high-resolution radiometers, and calculated the steric influences assuming a linear relationship (6 mm/℃) between SST and steric height (Sato *et al.*, 2001). Note that we can safely neglect the salinity influences of the steric height changes because these influences are much smaller than the temperature influences.

The ocean bottom pressure data from the ECCO model are available twice a day at 0 h and 12 h UTC on a 1° × 1° grid (Marshall *et al.*, 1997a, 1997b; Köhl *et al.*, 2002). The calculation was performed from January 1996 to December 1999.

2.2.3. Continental water loading influences

The continental water loads were estimated using the soil moisture data of Fan and van den Dool (2004). The data were prepared by assuming a one-layer "bucket" model based on reanalysis values for rainfall and temperature. The values were given in a 0.5° × 0.5° grid with the interval of one month. We calculated the displacements for the period from January 1996 to December 2004.

2.2.4. Snow loading influences

We used the snow depth data of the Automated Meteorological Data Acquisition System (AMeDAS). We calculated the influences from December 1997 to December 2001. Heki (2004) pointed out that the AMeDAS snow depth data tended to be underestimated because snow depths are highly dependent on altitudes, while AMeDAS observation points are spatially sparse and mainly installed along valleys for logistic reasons. In addition, snow density increases in spring due to compaction. Therefore, altitude correction and density correction are necessary before calculating the loading influences. For these corrections, we used 1.0° × 1.0° geometrical areas for convenient routine calculations, though Heki (2004) used the prefectures about district used by "altitude correction". In the other aspects of the corrections, we completely followed Heki (2004).

2.3. Comparison of the atmospheric loading influences

Although various loads were considered by several studies, only displacements due to

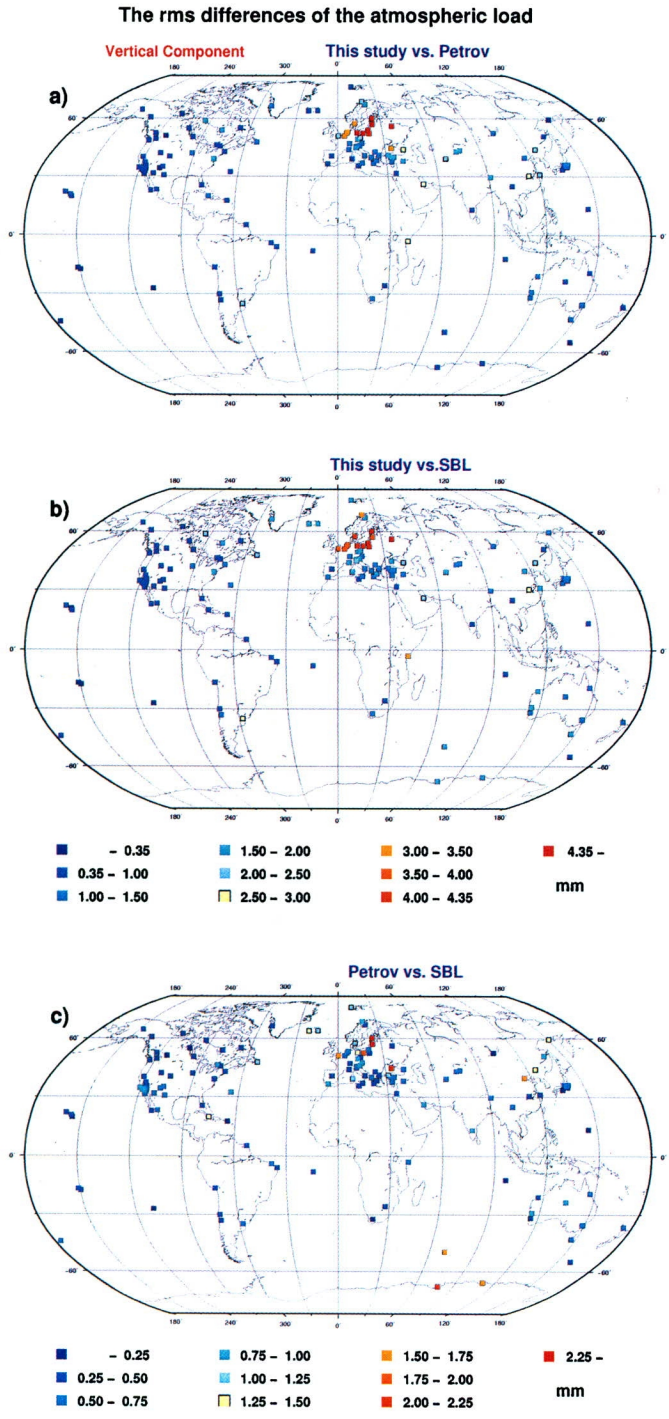

Fig. 1 The rms of differences (mm) of vertical displacements due to the atmospheric loads calculated by us (this study) and others (Petrov, SBL). a) This study vs. Petrov, and b) this study vs. SBL. The scales are shown under b). c) Petrov vs. SBL. The scale is shown underneath.

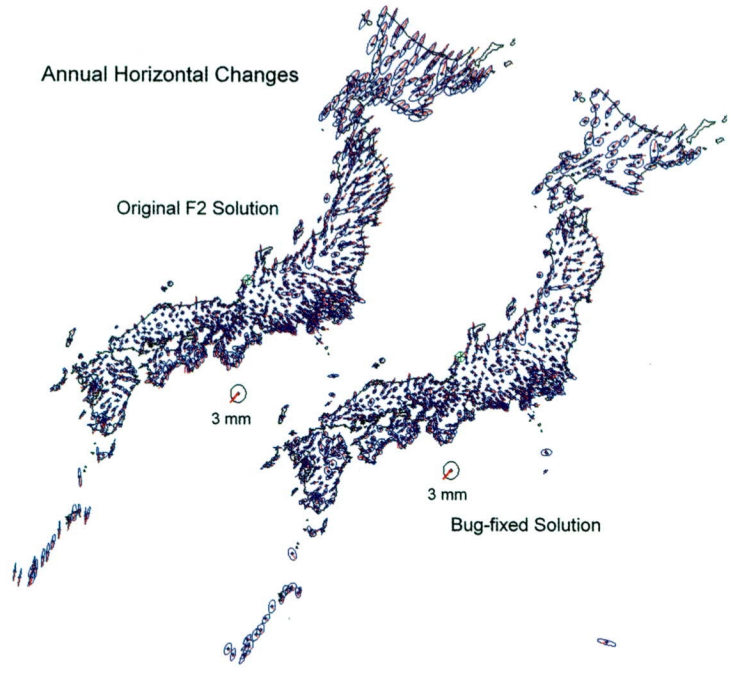

Fig. 2 Annual changes of horizontal GPS site coordinates. Left: the original F2 solution (similar to Figure 1 of Hatanaka (2003b)). Right: the bug-fixed solution. The blue ellipses show the locus of the annual horizontal change at each station with respect to the Komatsu station. The red lines show the time of summer of the annual locus.

atmospheric loads are provided as time series data at IGS observation points (Petrov and Boy, 2004; Gegout, 2004). Therefore, to evaluate our results, we compared them with those of the atmospheric loads at the IGS points. Note that Gegout (2004) routinely provides the time series as a service of the Special Bureau for Loading (SBL) of the International Earth Rotation and Reference Systems Service (IERS).

Figure 1 shows the root-mean-square (rms) differences of the time series of our results and those of Petrov and Boy (denoted as Petrov) and Gegout (denoted as SBL) at each observation point. In general, the rms differences are less than 0.2 mm in the horizontal components and less than 1.0 mm in the vertical component at most of the points. However, the rms differences in Europe, especially along the coast of the Baltic Sea, are rather large in both components. The main reason for the large differences is the resolution of the land-sea mask used for the calculations. While the resolution of the mask used by Gegout (2004) is not clear, Petrov and Boy (2004) used a $0.25^\circ \times 0.25^\circ$ mask. We used a $5' \times 5'$ ($0.083^\circ \times 0.083^\circ$) mask, and this difference might have resulted in the rms differences along the Baltic Sea coast. As pointed out by Kobayashi *et al.* (2004), the resolution of the land-sea mask is critical for coastal stations.

3. Correction of GEONET site coordinates

3.1. Time series of GEONET site coordinates

As the time series of GPS site coordinates, we used a routine solution of GEONET called the F2 solution, which was calculated using the Bernese software version 4.2 (Hatanaka *et al.*, 2003c). As previously mentioned, a software bug was found in the solid earth tide correction (Hugentobler, BSW mail #190, 2004). Because Tsukuba was fixed in the F2 solution, the error due to the bug is small near Tsukuba, but increases as the distance from Tsukuba increases. The maximum error is estimated to reach several millimeters at the farthest stations. Hatanaka (2004) showed a practical method to correct the errors, and we adopted his method to remove the errors in the F2 solution.

Munekane *et al.* (2004) pointed out that the time series of the coordinates at Tsukuba included the annual changes due to the groundwater variations of the surrounding areas. This means that the F2 solution calculated from the coordinates of Tsukuba as the reference includes the reverse signal due to the groundwater variations. Therefore, we changed the reference point from Tsukuba to Komatsu (ID: 950255) in this study. Strictly speaking, all the station coordinates should be re-analyzed using the Bernese software to eliminate the influences of the reference station. According to Beutler *et al.* (1989), the fixed station bias of 10 m introduces a scale influence of 0.4 ppm, and the estimated errors for all the GEONET stations are 0.3 mm at the 1,000-km baselines (Tobita *et al.*, 2003).

After moving the reference point to Komatsu, we further removed the trend and steps due to earthquakes and volcanic activities from the original time series. Finally, we used the time series of 892 stations that have long observation periods. Although the data used are from the beginning until the end of December 31, 2004, the loads were corrected according to the period of each of the load time series.

The annual changes of the horizontal coordinates (Komatsu fixed) before and after the bug in the Bernese software was fixed are shown in Figure 2. The whole network tended to expand in summer before the correction (Hatanaka, 2003b), but the tendency is hardly noticeable in the bug-fixed solution. Similarly, the annual changes of the vertical components were smaller in the bug-fixed solution.

3.2. Correction of the loading influences

Because we used the data sets of loading masses with time intervals from 12 hours to one month, we first interpolated all of the data sets to make them daily. Further, we applied a low pass filter to eliminate short period errors in both the loading influences and GPS time series. To determine the cut-off period of the low pass filter, we calculated the coherence between individual load time series and the time series of the GPS site coordinates (Figure 3). Strong correlations are commonly seen for periods from 200 to 400 days, as shown in Figure 3. The correlation values of the atmospheric loading influences are 0.8 to 0.9 for periods of around a year. On the other hand, very noisy features can be seen on timescales shorter than 100 days.

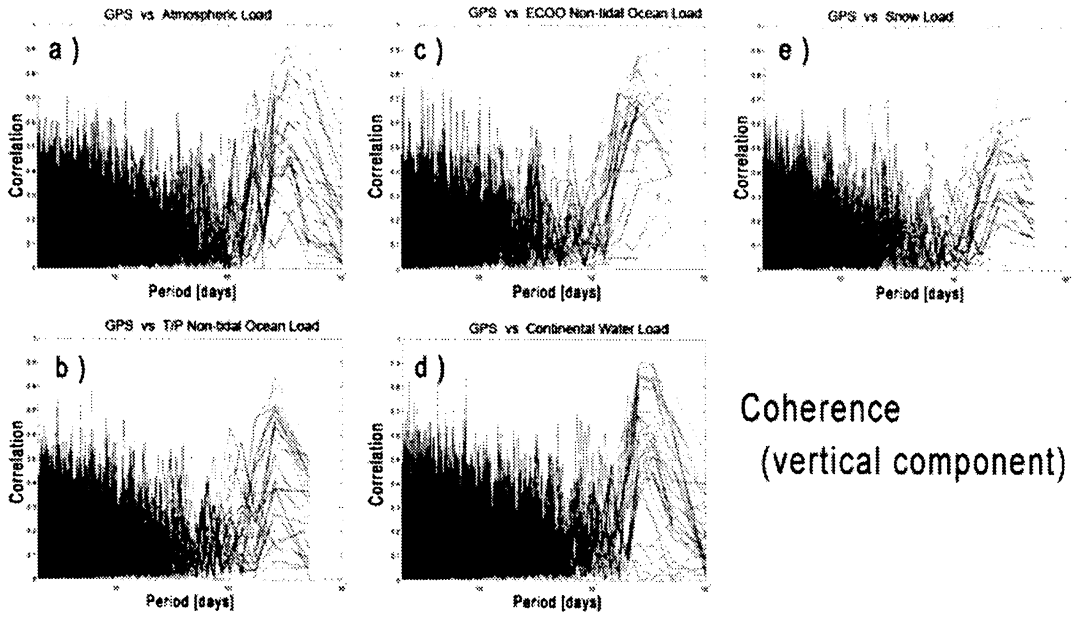

Fig. 3 The coherence of each load time series and GPS vertical site coordinate time series. a) GPS vs. AL, b) GPS vs. NTOL(T/P), c) GPS vs. NTOL(ECCO), d) GPS vs. CWL, and e) GPS vs. SL. The horizontal axis shows the period (in days). The vertical axis shows the correlation coefficient of the period.

Thus, we adopted 100 days as the cut-off period of the low pass filter.

The corrected time series were calculated as follows:

$$Corrected\ GPS = GPS - (Load_1 + Load_2 + \cdots + Load_n). \tag{3}$$

Actually, we calculated the following combinations of the loading influences:

case (1): $AL + NTOL(T/P) + CWL + SL$

case (2): $AL + NTOL(ECCO) + CWL + SL$

case (3): $AL + NTOL(T/P) + CWL$

case (4): $AL + NTOL(ECCO) + CWL$

case (5): AL only

case (6): $NTOL(T/P)$ only

case (7): $NTOL(ECCO)$ only

case (8): CWL only

case (9): SL only.

Cases (1) to (4) are intended to determine the combinations that can eliminate the load influences as much as possible. In these combinations, two ocean loads with and without SL are compared. Cases (5) to (9) are intended to estimate each of the loading influences. In general, some combinations of the data sets can more effectively eliminate the load influences as Takiguchi *et al.* (2006) suggested for precise Satellite Laser Ranging (SLR) data analyses.

3.3. Results

The results of the loading corrections are shown in Table 1 and Figure 4. To assess how well one can reduce periodic components by the corrections, we estimated the annual amplitudes and phases before and after the corrections using the least-squares method. The reduction rates of the annual amplitudes are shown in Table 1. Figure 4 shows an example of the time series of the displacements at station 950102 before and after the load corrections of cases (1) to (4). The phases are almost in harmony, although the amplitudes of the load contribution time series are smaller than those of the GPS time series.

The annual amplitudes decreased for all the cases except the vertical component of case (9), as shown in Table 1. The results show that the decrease percentages were about 15 to 30% in cases (1) to (4) except the vertical component of case (2). This means that the contribution of load influences such as the atmospheric, non-tidal ocean, and continental water loads in the periodic source of the GPS time series was about 20%. The results of cases (5)-(9) show that the influence of the non-tidal ocean load is larger than the others, especially in the horizontal components. This is not surprising considering that Japan is surrounded by oceans. NTOL (T/P) generally gave better results than NTOL(ECCO). The same results were obtained in a precise SLR analysis of an island area (Takiguchi *et al.*, 2006).

According to the comparison between cases (1) to (4) and (5) to (9), the decrease percentage was not additive, even if using plural loads, especially in case (2) for the vertical component. This might mean that the loads interact complexly. For example, common factors might be included in the source data, such as atmospheric pressure and sea level data.

3.4. Application to a slow slip event

We next checked whether the loading correction improved the accuracy of the GPS data processing for studying transient crustal deformations. For this purpose, we applied the loading corrections to a data set that included the 1997 slow slip event of the Bungo Channel region (Hirose *et al.*, 1999, Ozawa *et al.*, 2001). Following Hirose *et al.* (1999), we fixed Maebaru (ID: 950450) in the GPS analysis. For the comparison with the time series after loading correction, we prepared another time series empirically corrected for the secular trend, steps, and periodic changes using least-squares fittings. This time series was estimated as follows: 1) we estimated the parameters of the secular trend and the periodic changes only using the data after the event, and 2) using the parameters, we removed the periodic changes from the whole period of the data. We compared the obtained time series with the one corrected for the loading influences of case (4). The time series, which show good agreement, are compared in Figure 5. The rms differences between the two time series are summarized in Table 2. The differences are around 0.4 mm. This indicates that the correction of the loading influences worked well to eliminate the seasonal signals.

Hirose *et al.* (1999) and Ozawa *et al.* (2001) estimated the slip distribution on rectangular faults by using the inversion method of Yabuki and Matsu'ura (1992). In this case, using the time series corrected for load influences did not change the results very much because the rms

Table 1. The decrease percentage of annual amplitudes of the time series before and after the load correction. The mean value of each component in cases (1) to (9) is shown.

GEONET		NS (%)	EW (%)	UP (%)
case (1)	$AL+NTOL(T/P)+CWL+SL$	17.5	30.7	18.5
case (2)	$AL+NTOL(ECCO)+CWL+SL$	14.7	23.9	3.0
case (3)	$AL+NTOL(T/P)+CWL$	15.4	21.1	24.4
case (4)	$AL+NTOL(ECCO)+CWL$	14.5	17.8	17.7
case (5)	AL	9.0	9.4	15.9
case (6)	$NTOL(T/P)$	15.1	13.7	17.6
case (7)	$NTOL(ECCO)$	15.5	9.6	7.7
case (8)	CWL	7.2	8.5	4.4
case (9)	SL	8.4	15.2	−1.1

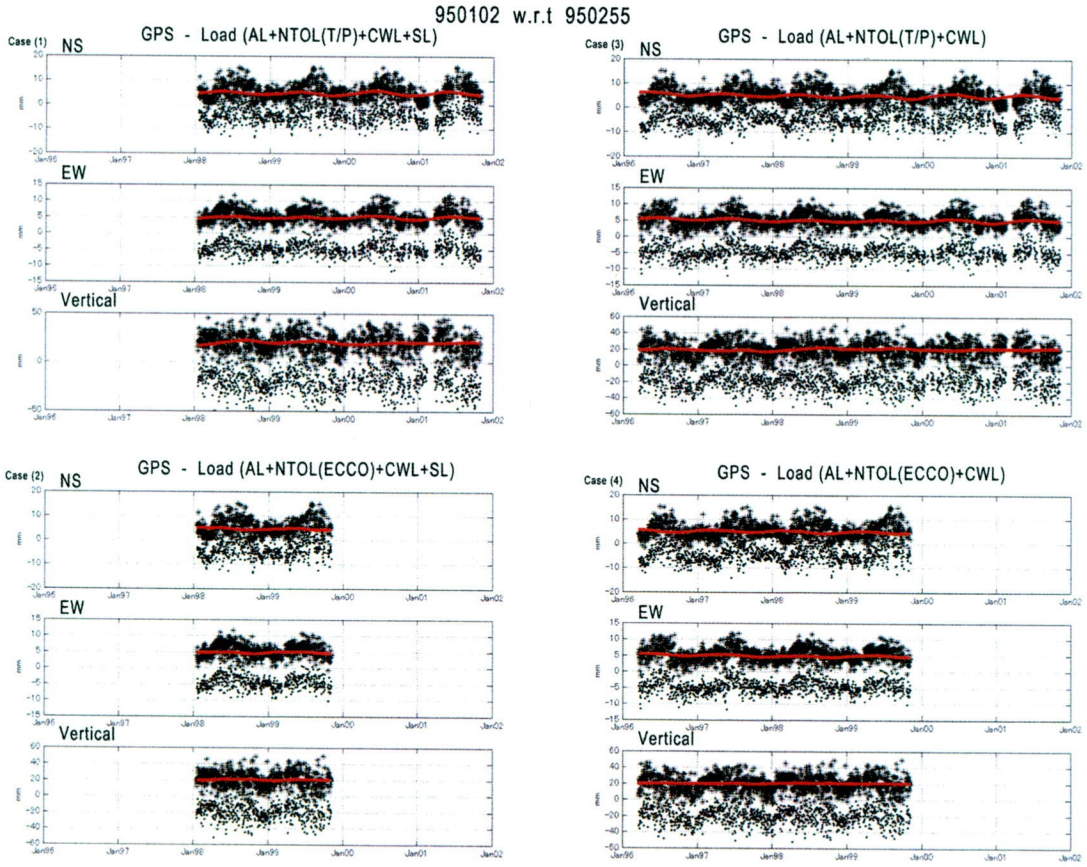

Fig. 4 GPS site coordinate time series before (black asterisks) and after (black dots) the load corrections at station 950102. The four panels correspond to cases (1) to (4) in the text. The red curves represent the time series of the total displacements caused by the loads.

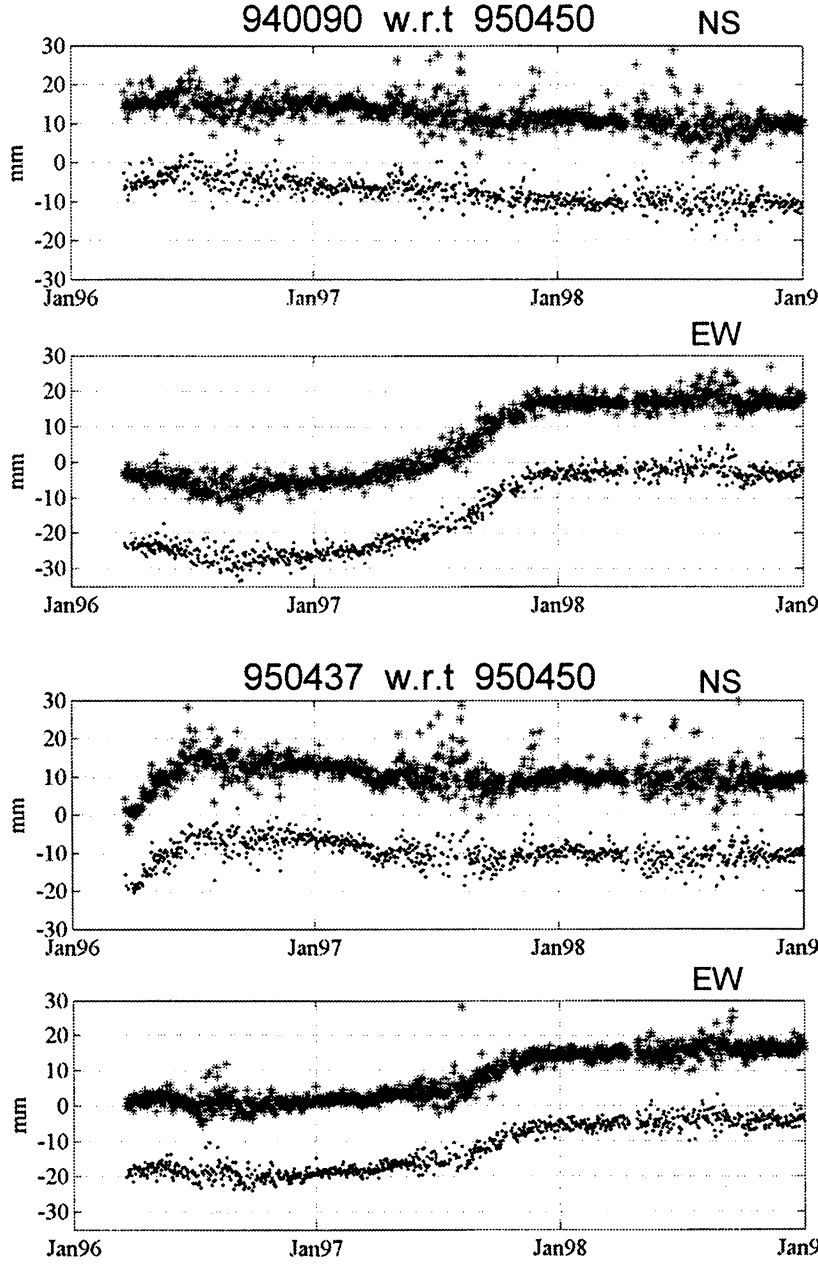

Fig. 5 Horizontal displacement time series at Ooitasaiki (940090) and Mishou (950437) from April 1996 to December 1999, with respect to Maebaru (950450). The black asterisks show the time series after the removal of periodic changes by using the least-squares method. The black dots show those after we removed periodic changes using the case (4) load correction.

Table 2. The rms of the differences of the coordinates between the two time series, one after the removal of periodic changes using the least-squares method, and the other after the load correction of the present study. In the first and third columns, the station IDs and the station names are listed. In the second column, the rms (mm) of the difference between the NS and EW components are listed.

Station ID	rms (mm)		Station Name
	NS	EW	
940090	0.91	0.31	Ooitasaiki
950437	0.41	0.44	Mishou
950447	0.18	0.37	Nishitosa
950449	0.27	0.39	Kohchiohtsuki
950466	0.32	0.30	Seiwa
950472	0.35	0.88	Yufuin
950473	0.25	0.41	Saganoseki
950474	0.40	0.30	Kujuu
950475	0.30	0.25	Ooitamie
950477	0.82	0.37	Hinokage
950478	0.52	0.41	Shiiba
950480	0.30	0.39	Kawaminami
mean	**0.42**	**0.40**	

differences were less than 1 mm. However, it is meaningful that the two conceptually very different (i.e. mathematical and physical) methods gave similar results. The benefit of the load correction might be well demonstrated if event profiles underwent, for example, unexpected periodic variation due to repeated slow slip events. In the future, the onset of the slow slip event and the slip rate would be determined more precisely by improving the time resolution of the changing loads.

4. Conclusion

We calculated the time series of the displacements of GEONET stations due to globally distributed surface loads, and found that an appropriate combination of the load-induced displacements accounted for the annual movements of GPS sites by up to 20%. The load correction using multiple loads was more effective than that with single loads, but the effect was not additive because the loads interact intricately. We also found that such loading correction can be applied for analyses of slow slip events. Periodic signals can be eliminated a posteriori, but this may inadvertently eliminate true signals. Our method based on a-priori knowledge is therefore meaningful. The loading correction could become more precise by improving the resolution and accuracy of the loading masses. This would be realized by satellite gravity data in the future.

Acknowledgements

We kindly acknowledge GSI, NCEP/NCAR, WOCE, NOAA, ECCO, and CPC for providing data used in our analysis (web addresses given below). We used the subroutines of GOTIC2 to calculate the load displacements. The public domain software Generic Mapping Tools by Wessel and Smith was used to prepare the figures in this paper. The comments by two reviewers, Prof. Teruyuki Kato and Prof. Kosuke Heki, and by the JGSJ Editor have significantly improved the manuscript.

[GSI (ftp://terras.gsi.go.jp/data/coordinates_F 2/), NCEP/NCAR (http://www.cdc.noaa.gov/), WOCE (http://podaac.jpl.nasa.gov/woce/), NOAA (http://www.cdc.noaa.gov/), ECCO (http://www.ecco-group.org/), CPC (http://www.cpc.ncep.noaa.gov/soilmst/leaky_glb.htm)]

References

Beutler, G., I. Bauersima, S. Botton, W. Gurtner, M. Rothacher and T. Schildknecht (1989): Accuracy and Biases in the Geodetic Application of the Global Positioning System, Manuscripta Geodaetica, **14**, 28–35.

Dong, D., P. Fang, Y. Bock, M. K. Cheng and S. Miyazaki (2002): Anatomy of apparent seasonal variations from GPS-derived site position time series, J. Geophys. Res., **107**, B4, 2075.

Fan, Y. and H. van den Dool (2004): Climate Prediction Center global monthly soil moisture data set at 0.5° resolution for 1948 to present, J. Geophys. Res., **109**, D10102.

Farrell, W. E. (1972): Deformation of the Earth by Surface Loads, Rev. Geophys. and Spac. Phys., **10**(3), 751–797.

Gill, A. E. and P. Niiler (1973): The theory of seasonal variability in the ocean, Deep Sea Res. Oceanogr. Abstr., **141**, 141–177.

Hatanaka, Y. (2003a): Seasonal variation of scale of GEONET network and ZTD biases, paper presented at the Symposium JSG01, 23rd IUGG General Assembly, Sapporo, Japan, July 7.

Hatanaka, Y. (2003b): Observation of crustal deformation and seasonal variation with GPS, "GEKKAN CHIKYU", **25**, 2, 103–108 (in Japanese).

Hatanaka, Y. (2003c): Improvement of the analysis strategy of GEONET, Bull. Geograph. Survey Inst., **49**, 11–37.

Hatanaka, Y. (2004): Re-evaluation of seasonal variations of scale in the GEONET solutions, 102nd meeting of the Geodetic Society of Japan Program and Abstracts, 71–72 (in Japanese).

Heki, K. (2001): Seasonal modulation of interseismic strain buildup in Northeastern Japan driven by snow loads, Science, **293**, 89–92.

Heki, K. (2003): Snow load and seasonal variation of earthquake occurrence in Japan, Earth Planet. Sci. Lett., **207**, 159–164.

Heki, K. (2004): Dense GPS array as a new sensor of seasonal changes of surface loads, in The State of the Planet: Frontiers and Challenges in Geophysics, edited by R. S. J. Sparks and C. J. Hawkesworth, Geophys. Monograph, **150**, 177–196, American Geophysical Union, Washington.

Hirose, H., K. Hirahara, F. Kimata, N. Fujii and S. Miyazaki (1999): A slow thrust slip event following the two 1996 Hyuganada earthquakes beneath the Bungo Channel, southwest Japan, Geophys. Res. Let., **26**, 21, 3237–3240.

Kobayashi, Y., S. Iwano and Y. Fukuda (2004): Detailed Coastline Data around Syowa Station, Antarctica, and Calculation of the Oceanic Tidal Loading Effects, J. Geod. Soc. Japan, **50**, 1, 17–26.

Köhl, A., D. Stammer, B. Cornuelle, E. Remy, Y. Lu, P. Heimbach and C. Wunsch (2002): The Global 1° WOCE Synthesis: 1992–2001, in ECCO Rep. Ser., Rep. No. **20**. Estimating the Circ. and Clim. of the Ocean, Jet Propul. Lab., Pasadena, Calif.

Kalnay, E., M. Kanamitsu, R. Kistler, W. Collins, D. Deaven, L. Gandin, M. Iredell, S. Saha, G. White, J. Woollen, Y. Zhu, A. Leetma, R. Reynolds, M. Chelliah, W. Ebisuzaki, W. Higgins, J. Janowiak, K. C. Mo, C. Ropelewski, J. Wang, R. Jenne and D. Joseph (1996): The NCEP/NCAR 40-Year Reanalysis Project, Bullet. Amer. Meteorol. Soc., vol. **77**, pp. 437–471.

Marshall, J., C. Hill, L. Perelman, and A. Adcroft (1997a): Hydrostatic, quasihydrostatic and nonhydrostatic ocean modeling, J. Geophys. Res., **102**, 5733–5752.

Marshall, J., A. Adcroft, C. Hill, L. Perelman and C. Heisey (1997b): A finite-volume, incompressible Navier-Stokes model for studies of the ocean on parallel computers, J. Geophys. Res., **102**, 5753–5766.

Mangiarotti, S., A. Cazenave, L. Soudarin and J. F. Cretaux (2001): Annual vertical crustal motions predicted from surface mass redistribution and observed by space geodesy, J. Geophys. Res., **106**, 4277–4292.

Matsumoto, K., T. Sato, T. Takanezawa and M. Ooe (2001): GOTIC2: A Program for Computation of Oceanic Tidal Loading Effect, J. Geod. Soc. Japan, **47**, 1, 243–248.

McCarthy, D. D. (ed.) (1996): IERS Conventions (1996), IERS Techn. Note, **21**, Obs. de Paris.

Munekane, H., M. Tobita and K. Takashima (2004): Groundwater-induced vertical movements observed in Tsukuba, Japan, Geophys. Res. Let., **31**, L12608, doi:10.1029/2004GL020158.

Ozawa, S., M. Murakami and T. Tada (2001): Time-dependent inversion study of the slow thrust event in the Nankai trough subduction zone, southwestern Japan, J. Geophys. Res., **106**, B1, 787-802.

Petrov, L. and J.-P. Boy (2004): Study of the atmospheric pressure loading signal in very long baseline interferometry observations, J. Geophys. Res., **109**, B03405.

Takiguchi, H., T. Otsubo and Y. Fukuda (2006): Mass-redistribution-induced crustal deformation of global satellite laser ranging stations due to non-tidal ocean and land water circulation, Earth, Planets and Space, **58**, e13-e16.

Tobita, M., H. Munekane, S. Matsuzaka, Y. Kuroishi, Y. Masaki and M. Kato (2003): Groundwater-Driven Vertical Movement in Tsukuba Detected by GPS (II), 100th meeting of the Geodetic Society of Japan Program and Abstracts, 67-68 (in Japanese).

Sato, T., Y. Fukuda and Y. Aoyama (2001): On the observed annual gravity variation and the effect of sea surface height variations, Phys. Earth Planet. Inter., **123**, 45-63.

van Dam, T. M. and T. A. Herring (1994): Detection of atmospheric pressure loading using very long baseline interferometry measurements, J. Geophys. Res., **99**, 4505-4518.

van Dam, T. M., G. Blewitt and M. B. Heflin (1994): Atmospheric pressure loading effects on Global Positioning System coordinate determinations, J. Geophys. Res., **99**, 23939-23950.

van Dam, T. M. and J. Wahr (1998): Modeling Environment Loading Effects: a Review, Phys. Chem. Earth, **23**, 9-10, 1077-1087.

van Dam, T., J. Wahr, P. C. D. Milly, A. B. Shmakin, G. Blewitt, D. Lavallee and K. M. Larson (2001): Crustal displacements due to continental water loading, Geophys. Res. Let., **28**, 4, 651-654.

Yabuki, T. and M. Matsu'ura (1992): Geodetic data inversion using a Bayesian information criterion for spatial distribution of fault slip, Geophys. J. Int., **109**, 363-375.